ELSEVIER

Dyes and Pigments 43 (1999) 207–217

DYES and PIGMENTS

Spin pairing ('dimerisation') of the viologen radical cation: kinetics and equilibria

Paul M.S. Monk*, Neil M. Hodgkinson[1], Saika A. Ramzan

Department of Chemistry and Materials, Manchester Metropolitan University, Manchester M1 5GD, UK

Received 6 April 1999; accepted 10 May 1999

Abstract

Viologen radical cations dimerise (spin pair) in aqueous solution, causing the colour of the viologen dye to alternate between blue (monomer) and dimer (red). Equilibrium constants K of viologen dimerisation have been determined using UV–vis spectroscopy for alkyl viologen radical-cation species in halide solutions. Equilibrium constants of dimerisation were obtained by deconvolution of optical spectra. Values of $\Delta G^{\circ}_{\mathrm{dim}}$ have a crude linear dependence on n, the length of the alkyl substituent chain, for $n = 2$ to 8. Rate constants of spin-pairing k_{dim} (i.e. dimerisation of the radical cation) have been determined. Bjerrum plots indicate that the rate-limiting reaction during dimerisation involves anions: it is postulated that the dimerisation reaction is two-step, with dimer formation occurring after the formation of an association pair comprising a radical cation and a counter anion. Recent comproportionation results are used to analyse the structure of the dimer and the role of anions during dimerisation. The possibility that dimer comprises anions placed between the planes of the two bipyridilium radicals is also discussed.

Keywords: Viologen; Bipyridilium; Kinetics; Radical cation; Dimerisation

1. Introduction

The viologens are salts of 4,4′-bipyridine [1]. Viologen salts are named formally as 1,1′-di(substituent)-4,4′-bipyridilium but usually termed 'substituent' viologen. They may exist in several redox forms. The redox state prepared or purchased is the dication, as conveniently made by Anderson [2] quaternisation of 4,4′-bipyridine with the relevant alkyl halide. The Anderson reaction is the aromatic analogue of the more familiar Menshutkin [3] reaction of aliphatic amines. Following quaternisation, the halogen atom becomes a halide counter anion within the viologen salt.

One-electron reduction of the dication yields an intensely-coloured dye, the paramagnetic viologen radical cation, reaction (1):

$$\mathrm{bipm}^{2+} + \mathrm{e}^{-} \rightarrow \mathrm{bipm}^{+\bullet} \quad (1)$$

where the source of the electron e^{-} is either an electrode or a chemical reductant such as zinc dust or dithionite ion. The radical dye is particularly stable, so its colour will persist almost indefinitely in the absence of oxidising agents such as oxygen.

* Corresponding author. Tel.: +44-(0)161-247-1421; fax: +44-(0)161-247-1438.

E-mail address: p.monk@mmu.ac.uk (P.M.S. Monk)

[1] Current address: Baxenden Chemicals Ltd., Accrington, Lancashire, BB5 2SL, UK.

0143-7208/99/$ - see front matter
PII: S0143-7208(99)00054-6

While the colour of the dye is stable and intense, its colour is not constant: the UV–vis spectra of alkyl bipyridilium radical cations in (dilute) aqueous solution typically show [4] a broad band at ca. 600 nm, the value of λ_{max} shifting in more concentrated solutions to lower wavelengths, with a new band appearing at ca. 900 nm. This phenomenon is ascribed to the formation of dimer [5] [Eq. (2)]:

$$2\,\mathrm{bipm}^{+\bullet} = (\mathrm{bipm})_2^{2+} \tag{2}$$

Dimerisation of viologen radicals in water is very common [1,6]. Since the dimer and monomer absorb in approximately the same spectral region, and both have roughly similar extinction coefficients, the colour of the radical cation (monomer or dimer) is not attributable to the *unpaired* electron. The colour of the dimer is in fact due to the new band at 900 nm, itself an allowed transition within the dimer, which is commonly stated to have a sandwich-type [4,5,7] structure with overlapping π-orbitals. The dimer is diamagnetic because opposing spins are paired [7].

The presence of dimer has sometimes been noted in previous work on viologen electrochromism [8,9], but in other studies it has caused only confusion [10,11]. Accordingly, we decided to characterise the radical cation dimer as a function of chain length *n*; surprisingly, values of λ_{max} and ε have not previously been published as a function of *n*.

We also report on a brief study to follow the rates of radical dimerisation. Unfortunately, not many rate constants exist in the literature, these few being $(1.0 \pm 0.2) \times 10^4$ (mol dm^{-3})$^{-1}$ s^{-1} for heptyl viologen [12], $(2.1 \pm 0.8) \times 10^5$ (mol dm^{-3})$^{-1}$ s^{-1} for octyl viologen [11], and a half life of 25 μs for benzyl viologen radical-cation monomer [13] [which equates to $k_{dim} = 1 \times 10^7$(mol dm^{-3})$^{-1}$ s^{-1}]. Compton et al. [14] have used in situ electrochemical electron paramagnetic resonance (EPR) spectroscopy to show that $k_{dim} > 10^5$ (mol dm^{-3})$^{-1}$ s^{-1} for methyl viologen (MV). Most recently, Compton et al. [15] found a lower value of $k_{dim} = 10^4$ (mol dm^{-3})$^{-1}$ s^{-1} for MV, and also noted $k_{-dim} = 30$ s^{-1}; this last analysis used a.c. impedance traces. All of these studies used water as solvent.

2. Experimental

Viologens were prepared by Anderson quaternisation of 4,4′-bipyridine (Aldrich) and the relevant alkyl halide in DMF. (Cold dimethyl sulphate (Fisons) was the alkylating agent used to prepare methyl viologen.) The appendix contains some sample preparative data.

Alkyl iodides were used when preparing short-chain viologens (propyl, butyl or pentyl) in consequence of the higher boiling temperature attainable for reflux; other halides were bromides. Iodide ion was replaced with bromide via ion exchange (with Duolite from BDH). Finally, all viologens were recrystallised from aqueous ethanol to yield yellow microcrystalline solids.

The chemical reduction of viologen dications was achieved using sodium dithionite (BDH) in cooled aqueous solutions. The SO_2 by-product of reduction was removed by entrapment within the N_2 gas used for sparging: solutions were de-oxygenated prior to addition of the reducing agent, and air was excluded from all solutions as the reaction between radical cation and molecular oxygen is particularly fast [16]. Solutions were subsequently equilibrated to (25 ± 0.3)°C. Cooling was necessary since warm dithionite will reduce bipm$^{+\bullet}$ further to form a di-reduced redox state, which we call bipm^{o} [17].

2.1. Determination of K_{dim}

Optical spectroscopy was performed with solutions in a thin cell of internal path length 1 mm and with a Philips PU-8720 spectrometer. A cell containing an aqueous solution of dithionite solution was used as the blank. Deconvolution was performed as follows: spectra were redrawn using an energy-related abscissa scale (υ in cm^{-1} being convenient). Bands thus redrawn were assumed to be gaussian and thus symmetrical about υ_{max}. A spreadsheet package (on Microsoft Excel) was used to compare the experimental results obtained with a model generated from the following normal distribution function:

$$f(x) = \frac{1}{\sigma\sqrt{2\pi}} \cdot \exp\left[\frac{-(x-\overline{x})^2}{2\sigma^2}\right] \tag{3}$$

which simplifies to

$$f(x) = A.\exp\{-B(x-\overline{x})^2\} \quad (4)$$

where

$$A = \frac{1}{\sigma\sqrt{2\pi}}$$

and

$$B = \frac{1}{2\sigma^2}$$

In this simplified form, $\overline{x}$ and σ have their usual statistical meanings of mean and standard deviation respectively. σ^2 is the variance. In this procedure, values of band half width are optimised till experimental and composite calculated bands are the same. Values of ε and λ_{max} for each of the two the spectroscopic bands (monomer and dimer) obtained via deconvolution are in good agreement with those in the literature [5,12,18].

The equilibrium constants of dimerisation K_{dim} were expressed as a function of optical variables via the Beer–Lambert law [Eq. (5)]:

$$K_{dim} = \frac{[\text{Dimer}]}{[\text{Monomer}]^2} = l \times \frac{A_D \varepsilon_{M^2}}{A_{M^2}\varepsilon_D} \quad (5)$$

where subscripts M and D refer to monomer and dimer respectively, l is the optical path length and the terms A are optical absorbances.

2.2. Determination of K_{dim}

Rate constants were determined using a previously-described procedure [6]. Solutions as above were placed in the path of a monochromated light beam. The wavelength λ_{probe} of 650 nm was chosen since only monomer is optically absorbing at this wavelength. The transmitted light was monitored with time following a ca. 10 μs pulse of white light (Helios 20 flash). The transmittance T of the solution was directly proportional to the millivolt output of a photomultiplier P, this voltage being recorded on a Gould 1425A 2072 digital oscilloscope. Plots of $f(P)$ against time were thus akin to simple kinetic spectra (vide infra).

The relative concentrations of dimer and monomer prior to photolytic perturbation, were calculated using K_{dim}.

3. Results

3.1. Spectra

Solutions of radical cation were blue–purple if n was small, and more red as n increased, thus indicating that the incidence of dimerisation increased with increasing n. Fig. 1 shows the deconvoluted UV–visible spectra of the radical cations of methyl viologen. The spectrum has been drawn with an energy-related abscissa in order for bands to be symmetrical (gaussian). The spectrum clearly contains several bands: that at λ_{max} 16,660 cm^{-1} (600 nm) is attributable to monomeric radical cation, and the band at 17,700 cm^{-1} (565 nm) is due to dimer. There are also a pair of very slight bands at 15,000 cm^{-1} (670 nm) and at ca. 21 000 cm^{-1} (480 nm). Their origin is unclear, as the spectrum of monomer and dimer both contain them. The spectrum of the dimer also contains a new band at ca. 900 nm.

3.2. Equilibrium constants

From spectra such as that in Fig. 1, values of λ_{max} and ε were obtained (see Table 1). Values of K_{dim} were determined spectroscopically using values of A and Eq. (5), and are listed in Table 2. The corresponding values of ΔG^o_{dim} were obtained using the van't Hoff isotherm as $-RT\ln(K_{dim})$. Such ΔG^o_{dim} values are included in Table 2. Values of ΔH^o_{dim} were obtained from isochore plots of $\ln(K_{dim})$ against $^1/T$; entropies of dimerisation ΔS^o_{dim} were obtained using $\Delta G^o_{dim} = \Delta H^o_{dim} - T\Delta S^o_{dim}$. These thermodynamic quantities are also included in Table 2.

It can be seen from Table 2 that values of ΔG^o_{dim} become less negative as the chain length increases. A plot of ΔG^o_{dim} against chain length n shows a linear portion from $n = 2$ to $n = 8$ (see Fig. 2) indicating that each $-CH_2-$ unit decreases the overall free energy by a set amount of about 1.6 kJ mol^{-1} per carbon.

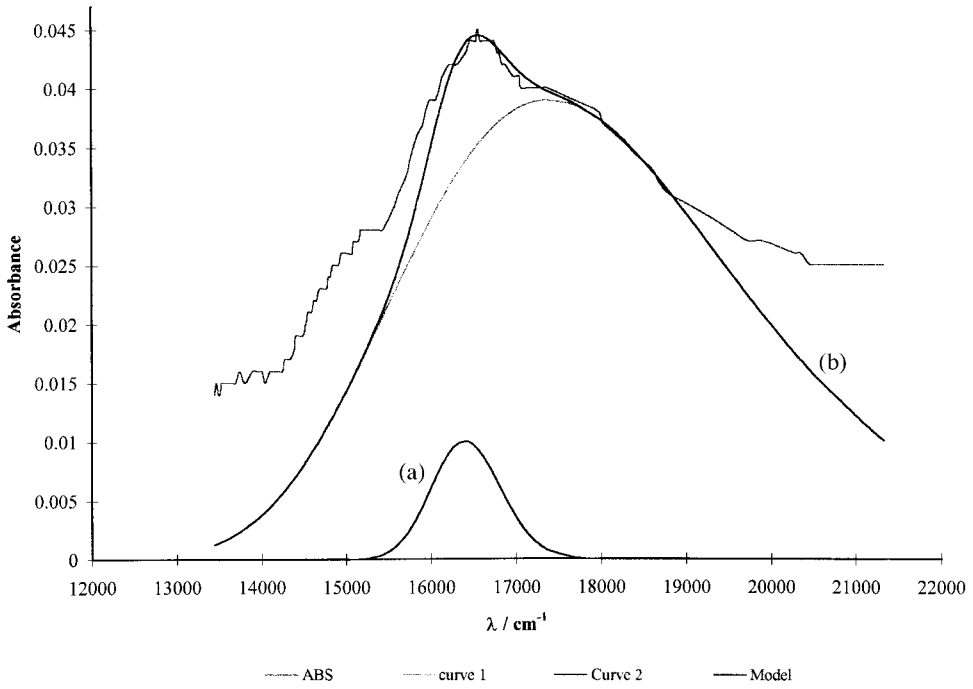

Fig. 1. UV–visible spectrum of an aqueous solution of methyl viologen radical cation. Methyl viologen was used as the methosulphate salt and reduction was performed using sodium dithionite. The bold line is the spectral band obtained experimentally and the faint lines are (a) monomer and (b) dimer.

Table 1
Spectroscopic properties of alkyl-viologen radical cations in water at 298 K as a function of substituent R[a]

R	Anion	λ_{max} (M[b])/nm	λ_{max} (D[b])/nm	ε (M)/M^{-1} cm^{-1}	ε (D)/M^{-1} cm^{-1}
Methyl	$MeSO_4^-$	598	551	13 700	8950
Ethyl	Br^-	597	564	12 200	8905
n-Propyl	Br^-	597	550	10 600	8870
n-Pentyl	Br^-	602	563	10 400	8690
n-Hexyl	Br^-	600	558	10 250	8700
n-Heptyl	Br^-	571	515	10 160	8560
n-Octyl	Br^-	548	504	8920	8550

[a] Values of λ_{max} were determined optically; values of ε were determined following computer deconvolution of optical data; the original concentration of viologen dication as 10^{-3} mol dm^{-3} in each case. Radical cation was formed by reduction with dithionite.
[b] Descriptors M and D refer to monomer and dimer, respectively.

3.3. Kinetics

The obtaining of rate constants will now be considered. During the flash experiments conducted here, the optical parameter determined was transmittance T, since photomultiplier output $P \propto T$. Absorbance A and transmittance T are related, viz. $A = \log(T_o/T)$, where T_o is the transmittance in the absence of optically-absorbing species and T is the transmittance when a chromophore, such as monomer or dimer viologen radical cation, is in the path of the beam. Note that the function A is proportional to $-\log(T)$ since T_o is a constant.

Absorbance A is proportional to concentration at 650 nm. The transmittance was measured at 650

Table 2
Equilibrium constants and changes in Gibbs function of viologen radical cation dimerisation in water at 298 K as a function of substituent R[a]

R	Anion	$K_{dim}/(mol\ dm^{-3})^{-1}$	$\Delta G^{\circ}_{dim}/kJ\ mol^{-1}$	$\Delta H^{\circ}_{dim}/kJ\ mol^{-1}$	$\Delta S^{\circ}_{dim}/J\ K^{-1}\ mol^{-1}$
Methyl	$MeSO_4$-	1.25×10^5	−29.1	−1.25	93.4
Ethyl	Br^-	1.08×10^5	−28.8	−4.21	96.9
n-Propyl	Br^-	4.85×10^4	−25.8	−1.15	92.8
n-Pentyl	Br^-	2.15×10^4	−27.7		
n-Hexyl	Br^-	7.05×10^3	−25.1		
n-Heptyl	Br^-	7.04×10^3	−22.0		
n-Octyl	Br^-	1.94×10^3	−18.8		

[a] Values of K_{dim} were determined spectroscopically (optical data were obtained spectroscopically and deconvoluted); concentrations were calculated using the optical data in Table 1 $[viologen]_{total} = 10^{-3}$ mol dm^{-3} in each case.

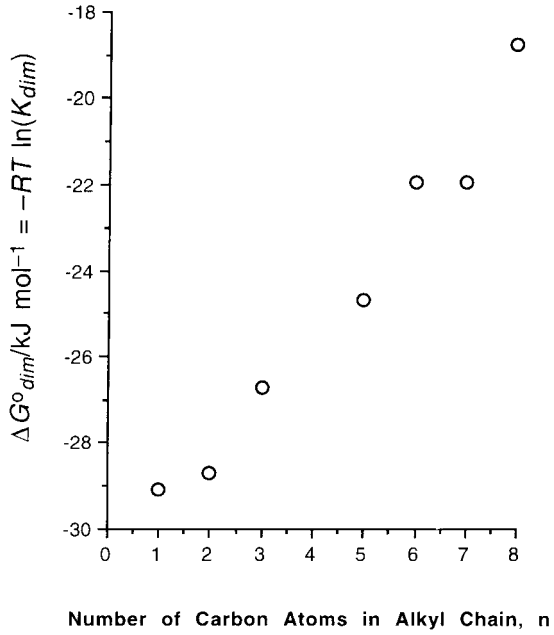

Fig. 2. Plot of ΔG°_{dim} against alkyl-chain length.

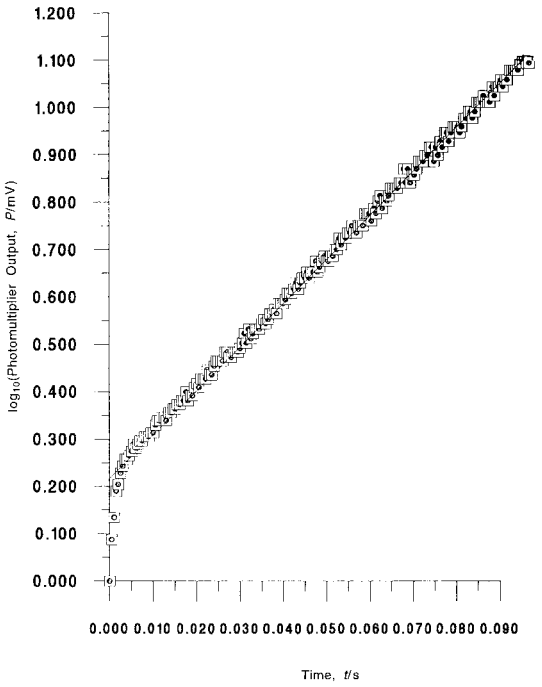

Fig. 3. Plot of log(T) against time for the propyl viologen radical cation in water. The increasing transmittance shows the proportion of monomeric radical decreasing with time following the flash.

nm, the wavelength being chosen owing to its being close to λ_{max} for the monomeric radical, but on the low energy side of the band in order to avoid the optical complications caused by overlapping of spectroscopic bands. Kinetic plots of $\log(A^{\infty} - A)$ against time are equivalent to $\log(\log(T^{\infty}|T))$ against time: such plots will be linear for first-order reactions and plots of $(A^{\infty} - A)^{-1}$ against time will be linear if the reaction is second-order.

Fig. 3 shows such a trace of log(P), i.e. transmittance T, as a function of time, in this case for propyl viologen radical cation in aqueous solution at 298 K. The time $t = 0$ corresponds to the commencement of the flash. The transmittance is seen to increase with time, implying that the proportion of radical existing as monomer decreases after the flash, i.e. dimer is forming at the expense of monomer.

Assuming that $k_{obs} = k_{dim}[monomer]^2 + k_{-dim} \times [dimer]$, i.e. assuming Eq. (2) as written, plots of

$^1/(A^\infty - A)$ as "$1/\log(T/T^\infty)$" against time were drawn, but in this study they were never linear, i.e. the reaction was not a straightforward second-order process. Also, it must be noted that no plots of observed rate against [radical]^2 were linear, as would have been required for a simple second-order reaction.

Similarly, plots of $\ln(\log(T/T^\infty))$ against time were non-linear, although they were only slightly curved, possibly implying a pseudo first-order process, (see below). The observed rate constant k_{obs} decreased very slightly as the the anion concentration increased, implying ionic complications.

Accordingly, a Bjerrum plot of log k_{dim} against $\sqrt{I}$ was drawn to investigate how ionic strength affected the dimerisation rate, e.g. to investigate whether ion-pairing to form neutral [bipm$^+$•X$^-$] species was kinetically relevant (Fig. 4). The gradient of a Bjerrum plot [20] is $(2A|Z_A Z_B|)$, where Z terms relate to the charges on reacting species A and B. The constant A is the familiar Debye–Hückel 'A' factor of 0.509. From the theory of Bjerrum–Bronsted, the gradient of a Bjerrum plot for a simple $(+1)(+1)$ reaction should be 1.02. Actually, the slope was negative, with a gradient of $-(0.94 \pm 0.05)$, implying that the reactants had charges of $+1$ and -1 (the ionic strength I was adjusted using KCl, a 1:1 electrolyte). When the supporting electrolyte was sulphate, the Bjerrum slope was almost doubled relative to that obtained with chloride as electrolyte, and when phosphate was the anion the slope increased by a factor of 2.5 (all gradients still retaining their negative slopes).

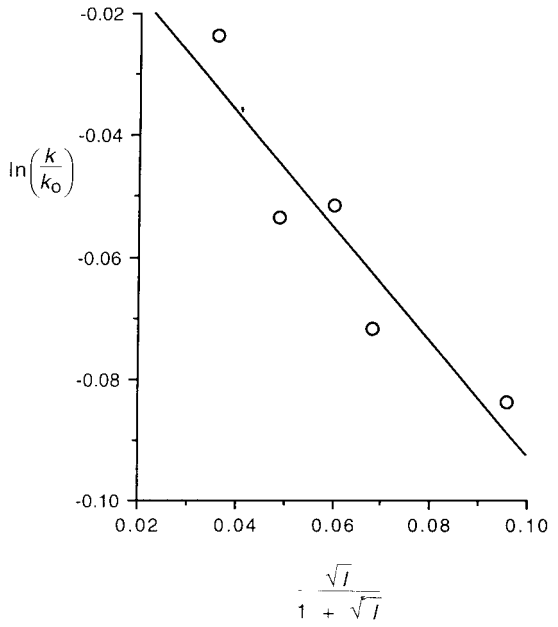

Fig. 4. Bjerrum plot of $\log_{10}(k/k_o)$ against (ionic strength, $I)^{1/2}$. The rate constant k_o refers to the rate constant obtained by extrapolation to zero ionic strength.

The rate constants k_{obs} are pseudo first order, thus explaining why first-order plots showed curvature. Two competing anionic effects were evinced: k_{obs} decreased with increasing $I^{1/2}$ according to the Bjerrum theory, but also increased with c (note that $c \propto I$ for a 1:1 electrolyte) since k_{obs} is pseudo first order-rate constant.

Values of k_{obs} must be converted into true second-order rate constants, e.g. dividing k_{obs} by the anion concentration. Values of k_{obs} at zero ionic strength were determined from plots such as shown in Fig. 4. Assuming the concentration of dimer to be small straight after the flash, values of k_{dim} were readily determined, and are listed in Table 3. Note that values of k_{dim} for $n > 5$ could be suspect, since it is known that considerable ion–cation association is present for these viologens causing the solubility limit to be reached; the solubility constant K_s for heptyl viologen bromide in water has been estimated by conductance methods to be 3.9×10^{-7} (mol dm^{-3})^2 [19].

Table 3
Rate constants of viologen radical cation dimerisation in water at 298 K as a function of substituent R[a]

R	Anion	k_{dim}/ (mol dm^{-3})$^{-1}$ s^{-1}	Lit. value	Ref.
Methyl	$MeSO_4$-	12.6×10^5		
Methyl	Cl^-		$>10^5$	[14]
Methyl	Cl^-		$>10^4$	[15]
Ethyl	I^-	9.0×10^5		
n-Propyl	Br^-	8.3×10^5		
n-Pentyl	Br^-	1.1×10^5		
n-Hexyl	Br^-	0.88×10^5		
n-Heptyl	Br^-	1.6×10^5	1.02 ± 10^4	[12]
n-Octyl	Br^-	1.0×10^5	2.1 ± 10^5	[12]

[a] All values have been adjusted to zero ionic strength.

Finally, as an adjunct, a Marcus-type plot of ΔG^{o}_{dim} (obtained via $-RT\ln K_{dim}$) against $\Delta G^{\ddagger}$ (via $-RT\ln k_{dim}$) was drawn (see Fig. 5). It is quite difficult to see a linear relationship in this figure, so it is implied that the rate measured does not relate to dimerisation per se, but to a separate process involved in the dimerisation reaction.

4. Discussion

Comparison of the values reported here with those in the literature is fairly difficult owing to the strong dependence on anion and ionic strength. For this reason, it is regrettable that data from some sources does not allow for ready comparison. For octyl viologen, the literature and experimental results respectively are 2.1×10^{5} (mol dm^{-3})$^{-1}$ s^{-1} and 1.0×10^{5} (mol dm^{-3})$^{-1}$ s^{-1}, which is satisfactorily close. For heptyl viologen, our rate constant of $k_{dim}=(1.6\pm0.2)\times10^{5}$ (mol dm^{-3})$^{-1}$ s^{-1} at $I=0$ is 16 times faster than the literature value [11] of 1.02×10^{4} (mol dm^{-3})$^{-1}$ s^{-1} (at unspecified ionic strength). The agreement for methyl viologen could be worse still if Compton's [15] smaller value of k_{dim} is accepted (he used 0.5 mol dm^{-3} NaCl as supporting electrolyte).

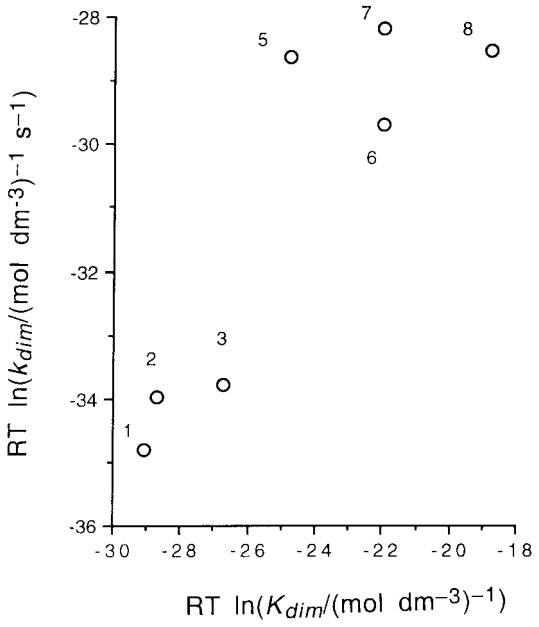

Fig. 5. Plot of ΔG^{o} against $\Delta G^{\ddagger}$ (both terms relating to dimerisation) in water at 298 K. The numbers relate to the number of carbon atoms in the *n*-alkyl chains.

The two values of k_{dim} in Ref. [12] are quoted for solutions comprising 10^{-5} mol dm^{-3} viologen and 0.1 mol dm^{-3} tris buffer at pH 8.1. Ion–ion interactions are thus more likely to be extensive (and uncompensated for) in Ref. [12], and the concentration of dithionite used in Ref. [12] is never specified, so perhaps a more considered comparison is not feasible.

We infer from the kinetic data above that the rate-limiting reaction during radical dimerisation occurs between an anion and a radical-cation monomer to form an association pair. This result necessitates the proposition of a new two-step mechanism for the viologen dimerisation reaction: first, a radical-cation monomer associates slowly with an anion [Eq. (6)]:

$$\mathrm{bipm}^{+\bullet} + \mathrm{X}^{-} \rightarrow \mathrm{bipm}^{+\bullet}\mathrm{X}^{-} \qquad (6)$$

which is followed by a more rapid spin-pairing reaction [Eq. (7)]:

$$2\mathrm{bipm}^{+\bullet}\mathrm{X}^{-} \rightarrow (\mathrm{bipm})_2^{2+}2\mathrm{X}^{-} \qquad (7)$$

It is clearly possible that Eq. (7) could proceed with only one of the radicals existing as an ion-paired monomer, so the other can be free [Eq. (7a)]:

$$\mathrm{bipm}^{+\bullet} + \mathrm{bipm}^{+\bullet}\mathrm{X}^{-} \rightarrow (\mathrm{bipm})_2^{2+}\mathrm{X}^{-} \qquad (7a)$$

although it must be noted that this variant still requires Eq. (6) to be the rate-limiting step.

The usual configuration stated for the dimer is a sandwich-type structure [4,5,7] with the two bipyridilium planes lying parallel and face-to-face. The validity of this structure — with both pyridinium rings overlapping completely — is attested by the way cyclopyridinophane species (e.g. structure **I**), when reduced, form analogous dimer species; cyclopyridinophanes (e.g. [21]) comprise two viologen moieties separated by a short, flexible alkyl or aryl linkages at either nitrogen.

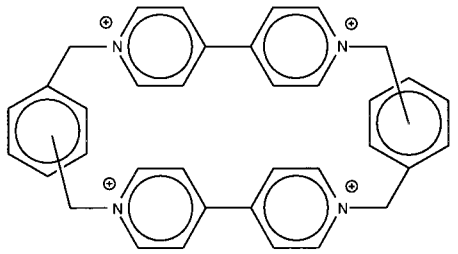

I

Dimerisation is favoured in aqueous solution alone (monomer being the predominant form in all organic solutions except at very low temperatures) [7]. This observed stability arises (in part, at least) from the rather large dispersion forces engendered when bulky molecules are positioned close together [22]. If dispersion forces were the sole consideration, however, then dimerisation would occur in other solvents than water. It is therefore suggested that the energetic contributions from increased water–water interactions (inevitable since two radical ions now occupy a single solvent cavity) are sufficient to overwhelm the repulsive coulombic forces apparent when two cations are close together.

The entropy changes in Table 2 are rather surprising since a *negative* entropy of dimerisation would be the expected result. A positive value of ΔS has also been observed, though in the case for the dimerisation of a series of alkyl-substituted viologens dissolved in methanol [7], greater freedom of solvent movement was postulated to occur on dimerisation in a similar manner to that observed during micellation. Since water (the solvent in the study here) is more strongly solvating than is MeOH, greater ΔH solvent–shell reorganisation energies will be involved during reaction in water. Also, the study here used longer alkyl chains then those of Evans et al. [7]. The changes in entropy which dominate the reaction are caused by solvent molecules gaining freedom when released during reaction.

The magnitude of the positive ΔS_{dim} terms gives an indication of the dimer structure [7]: for $\Delta S^{\mathrm{o}}_{\mathrm{dim}}$ to be so large, both radical monomers must be held within a small solvent-bound cavity since many water molecules have been released, i.e. the dimer must be plane-to-plane with a significant extent of π-orbital overlap.

The linearity of Fig. 2 is interesting. We presume that values of $\Delta H^{\mathrm{o}}_{\mathrm{dim}}$ are almost independent of substituent and that each $-CH_2-$ unit contributes a modicum of entropy to the overall thermodynamics of the association process (since a longer chain implies greater solvent reorganisation). A similar study by Evans et al. [7] used simple alkyl viologens but with MeOH as solvent. The data from these workers, when plotted, shows a similar trend, with $\Delta H^{\mathrm{o}}_{\mathrm{dim}}$ being proportional to chain length, each $-CH_2-$ contributing ca. 2 kJ mol^{-1}. A plot of $\Delta S^{\mathrm{o}}_{\mathrm{dim}}$ for viologens in MeOH against chain length was linear [7]. (While these trends are explicit, such graphs appear never to have been plotted.)

4.1. The role of anions

The kinetic process followed optically was dimerisation, but the rate-limiting process was clearly the formation of an association-pair between bipm$^{+\bullet}$ and X^- *prior* to the dimerisation reaction.

That the kinetics of the dimer-formation process depends on the anion in solution is not unlikely. Indeed, van Dam and Ponjeé [19] postulated in 1974 that the dimer has the anion placed *between* the two bipyridilium planes, though nowhere do they state the reasoning behind their assertion. Configurations with anion incorporation will be designated as (bipm–X–bipm)$^{2+}$.

Species of the type (bipm–X–bipm)$^{2+}$ have been prepared using comproportionation of viologen species [8,23] (vide infra, where we discuss the possibility that the rate of dimer formation depends on anions because species such as (bipm–X–bipm)$^{2+}$ were formed).

4.2. Viologen comproportionation and the role of counter anions in dimer structure

The comproportionation reaction of viologen species involves dication and another (uncharged) redox state—the dihydro viologen bipm$^{\mathrm{o}}$:

$$\mathrm{bipm^{o}} + \mathrm{bipm^{2+}} \rightarrow 2\mathrm{bipm^{+\bullet}} \qquad (8)$$

It is now fairly well established that the intermediate for this *redox* reaction is a radical-cation dimer [9]. Some of the dimer dissociates soon after formation (to fulfil thermodynamic criteria, e.g. equilibrium-constant constraints).

Recent additional data concerning the comproportionation of heptyl viologen in the presence of the bulky ferrocyanide anion [8], and previous data [23] concerning comproportionation of the aryl-substituted viologen 1,1′-*bis*(*p*-cyanophenyl)-4,4′-bipyridilium in the presence of $[Fe(CN)_6]^{4-}$, allow the inference that the $[Fe(CN)_6]^{4-}$ anion lies *between* the two bipyridilium planes during the electron-transfer stage of the comproportionation reaction. In the presence of ferrocyanide, the colour of dimer is not seen during comproportionation; electron transfer [Eq. (8)] does occur since the colour of *monomer* is seen instead.

At first sight, this result seems to contradict the above, but a slightly different comproportionation reaction mechanism is sufficient to explain the difference, as below. The incorporation of an anion during comproportionation is almost to be expected since viologen dications are quite electron poor and readily form charge-transfer complexes [24]. As an example, the association constant for the formation of a complex between MV^{2+} and $[Fe(CN)_6]^{4-}$ is [25] 52.4 $(\text{mol dm}^{-3})^{-1}$, and thus a large fraction of the MV^{2+} from the bulk solution can be expected to be associated with a donor anion during reaction with electrogenerated MV^{o}. Anion incorporation will occur if the anion is on the reacting face of the MV^{2+} moiety.

When a dimer species incorporating $[Fe(CN)_6]^{4-}$ is formed, it must either dissociate immediately (as only the colour of monomer is seen) or have $bipm^{+\bullet}$ planes positioned sufficiently far apart that no spin pairing is possible.

If monomer is seen because of rapid (perhaps catalysed) dissociation, then it is likely that part of the impetus for dissociation following comproportionation comes from thermodynamic considerations, since the concentration of dimer at the electrode interface is higher than warranted by K_{dim}.

Such thermodynamic consideration would not explain the *total* absence of dimer, hence the suggestion of the second reason for absence of dimer in that study, viz. the electron transferred from $bipm^{\circ}$ to $bipm^{2+}$ during comproportionation is transferred via an anion 'bridge' in an inner-sphere type of mechanism. The product 'dimer' $(bipm–X–bipm)^{2+}$ has its two viologen planes parallel, but if the anion is large, e.g. $[Fe(CN)_6]^{4-}$, the two viologen radicals are too far apart for the viologen orbitals to overlap, as required for spin pairing. Accordingly, the colour seen on comproportionation in the presence of anions such as $[Fe(CN)_6]^{4-}$ is that of monomer [8].

If, however, the counter anion X during comproportionation were smaller, e.g. chloride, then incorporated X in the $(bipm–X–bipm)^{2+}$ dimer would allow the two radical planes to get closer, thus engendering a sufficiently large overlap to provide the observed dimer stability and hence the colour of dimer.

Finally, if two monomer species approach and orbital overlap occurs *without* anion incorporation between the two $bipm^{+\bullet}$ units—as would be expected in the absence of comproportionation—then the expected coulombic repulsion between the two $bipm^{+\bullet}$ units will be greater because they will be closer without an intercalated anion, but the spin pairing energy will also be enhanced.

4.3. Solid state structures

There are no solid state X-ray structures of viologen radical cations in the literature. Concerning charge-transfer adducts of viologen dication (within which the extent of charge transferred in the ground state is never more than ca. 0.1 electrons [26]) the dication is similar to the viologen radical in being planar. XRD structures show the donor anion usually residingz close to the nitrogens of the pyridinium rings. Structures in the literature include:

1. complexes between TCNQ as donor and, as acceptors, symmetrical viologens having substituents such as *p*-cyanophenyl [27], methyl [28], ethyl [29];
2. complexes between methyl viologen and donors of chloride, bromide and iodide [30], quinol (in the presence of iodide as a counter ion) [31]; and
3. polyhalometallate complexes, e.g. between methyl viologen and [32] $CuCl_4^{2-}$ or between

protonated 4,4′-bipyridilium with [33] $Cu_2Cl_6^{2-}$. We have tried unsuccessfully to grow large crystals of methyl viologen radical cation for XRD analysis.

None of the published projections shows an anion *between* the planes. Also, it can be noted that none of the projections in Refs. [27–29] (which all pertain to complexes with the bulky TCNQ donor) show viologen units either close enough for interaction or with the molecular planes overlapping—surely a prerequisite for orbital overlap—although a few do show the viologen planes in a parallel, albeit staggered, configuration.

While no solid state X-ray structures exist for radical cations, a few studies of $MV^{+\bullet}$ have been performed using FTIR. In the work by Poizat et al. [34] it is explicitly stated that FTIR bands owing to dimer $(MV)_2^{2+}$ are clearly visible in the spectrum of solid state $MV^{+\bullet}$ Cl− but no additional structural details, for example the geometry within the dimer, are mentioned by these authors.

In the FTIR study by Hester and Suzuki [35], it is clear that force constants for the methyl groups of methyl viologen are anomalous: there is "a surprisingly large change in the CH_3 symmetric deformation accompanying the transformation (i.e. reduction) from MV^{2+} to $MV^{+\bullet}$ [35]." We take this effect to arise from dimerisation in the solid state. There is no mention of intercalation of anions, and their simulations ignore the presence of anions.

Finally, it is worth noting that both Evans et al. [7] and Symons et al. [22] detected an unknown paramagnetic species in solutions of methyl viologen radical cation. We suggest that this species is none other than bipm–X–bipm^{2+} in which X is sufficiently large that no spin pairing is possible.

5. Conclusion

Rates and equilibria of the spin pairing (dimerisation) of viologen radical cation monomers have been determined using flash photolysis and UV–vis spectroscopy. Equilibrium constants are quite large, thus demonstrating the stability to be gained on radical-spin pairing. The rate constants of dimerisation are quite fast. It is shown that some of the results, e.g. those obtained during viologen comproportionation, are best explained in terms of a dimer having an anion X placed between the two viologen units as (bipm–X–bipm)$^{2+}$. Species such as (bipm–X–bipm)$^{2+}$ have *only* been observed in such cases. Normal dimer is likely to have a straightforward $\pi-\pi$ structure, with anions electrostatically attached to the *outside* of the dimer assembly.

It is concluded that the dimerisation results obtained here, and obtained using dimer formed as the product of viologen comproportionation, are not incompatible since the latter dimer is probably different in terms of structure.

Acknowledgements

We wish to thank the Faculty of Science and Engineering at the MMU for granting a studentship to N.M.H.

Appendix. Sample syntheses of viologen species

Two methods of viologen preparation were employed during this study: methyl viologen was prepared with dimethyl sulphate as a methylating agent, and other viologens were prepared with an alkyl halide as the alkylating agent. As sample preparations, we give the syntheses of methyl viologen to illustrate the former method and of heptyl viologen to illustrate the latter.

A.1. Methyl viologen

Methyl viologen dication was prepared as the *bis*(methosulphate) salt by dissolving 4,4′-bipyridine (Aldrich) with excess dimethyl sulphate (Fisons) in dry DMF at room temperature. Crystals were apparent after ca. 2 h. Recrystallisation from cold aqueous ethanol produced white needle-like crystals in quantitative yield.

The purity of the methyl viologen was confirmed by the following data:

^{1}H NMR	$\delta = 9.1$ ppm, d of d, 4H (bipyridine); 8.5 ppm, d of d, 4H (bipyridine); 4.6 ppm, s, 6H, (Me) and 3.7 ppm, s, 6H, ($MeSO_4^-$).
^{13}C NMR	$\delta = 153$ ppm (Carbon-2);149 ppm (C-4); 129 ppm (C-3); 58 ($MeSO_4^-$) and 51 ppm (Me)
IR	3200 cm^{-1}, C-H; 1650 cm^{-1}, C=C, C=N; 1600, 1540, 1430 cm^{-1} (C=C); 1200, 1080 cm^{-1}; 880 cm^{-1}.
m.p.	decomposed at T > 270°C.

A.2. Heptyl viologen

A mixture of 4,4′-bipyridine (40 g, 0.256 molz) and 1-bromoheptane (40 g, 0.223 mol) in DMF were refluxed while stirring for 3 h. The resultant red solution was allowed to cool, and the precipitate filtered off. This crude product was recrystallised from aq. ethanol and then from acetonitrile to yield yellow plate-like crystals of $HV^{2+}2Br^-$ in 93% yield.

The purity of the heptyl viologen was confirmed by the following data:

^{1}H NMR	(Solvent = D_2O; reference = SSPA) $\delta = 0.89$ (t, CH_3); 1.1–2.4 (m, CH_2), 4.79 (t, N-CH_2); 8.61 (bipyridine); 9.18 ppm (bipyridine).
IR	(KBr)/cm^{-1} as $\upsilon_{max} = 3420$ (C−H), 1640, 1460 (C=C, C=N); 850, 815

Other viologens were prepared similarly but by reacting 4,4′-bipyridine with the relevant alkyl halides in an Anderson reaction [2].

References

[1] Monk PMS. The viologens: physicochemical properties, synthesis and applications of the salts of 4,4′-bipyridine. Chichester, UK: John Wiley and Sons Ltd, 1998.
[2] Anderson T. Liebig's Ann Chem 1855;94:358.
[3] Menshutkin N. Z Phys Chem 1890;5:589.
[4] Schwartz Jr, W. Ph.D. thesis, University of Wisconsin, WI, 1962, as cited in Ref. [5].
[5] Kosower E, Cotter JL. J Am Chem Soc 1964;86:5524.
[6] Bard AJ, Ledwith A, Shine HJ. Adv Phys Org Chem 1976;13:155.
[7] Evans AG, Evans JC, Baker MW. J Chem Soc, Perkin Trans 2 1977;1787.
[8] Monk PMS. J Electroanal Chem 1997;432:175.
[9] Monk PMS, Fairweather RD, Ingram MD, Duffy JA. J Chem Soc, Perkin Trans 2, 1992;2039.
[10] Kim SH, Bae JS, Hwang SH, Gwon TS, Doh MK. Dyes and Pigments 1997;33:167.
[11] Monk PMS. Dyes and Pigments 1998;39:125.
[12] Claude-Montigny B, Merlin A, Tondre C. J Phys Chem 1992;96:4432.
[13] van Leewen JW, van Dijk C, Veegar C. Eur J Biochem 1983;135:601.
[14] Webster RD, Dryfe RAW, Eklund JC, Lee C-W, Compton RG. J Electroanal Chem 1996;402:1647.
[15] Rueda M, Compton RG, Alden JA, Prieto F. J Electroanal Chem 1998;443:227.
[16] van der Leest RE. J Electroanal Chem 1973;43:257.
[17] Cairns JE, Carey JE, Colchester JE. J Chem Soc, Chem Commun 1969;1290.
[18] Bird CL, Kuhn AT. Chem Soc Rev 1981;10:49.
[19] van Dam HT, Ponjeé JJ. J Electrochem Soc 1974;121:1555.
[20] Logan SR. Fundamentals of chemical kinetics. Harlow: Longmans, 1996. p. 93
[21] Neta P, Richoux M-C, Harriman A. J Chem Soc, Faraday Trans 2 1985;81:1427.
[22] Blandamer MJ, Brivati JA, Fox MF, Symons MCR, Verma GSP. Trans Faraday Soc 1967;63:1850.
[23] Compton RG, Monk PMS, Rosseinsky DR, Waller AM. J Chem Soc, Faraday Trans 1990;86:2583.
[24] Monk PMS, Hodgkinson NM. Electrochim Acta 1998;43:245.
[25] Nakahara A, Wang JH. J Phys Chem 1963;67:496.
[26] Murthy ASN, Bhardwaj AP. Spectrochim Acta 1982;38A:207.
[27] Ashwell GJ, Cross GH, Kennedy DA, Nowell IW, Allen JG. J Chem Soc, Perkin Trans 2, 1983;1787.
[28] Ashwell GJ, Wallwork SC. Acta Crystallogr 1979;B35:1648.
[29] Ashwell GJ, Eley DD, Wallwork SC, Willis MR. Proc R Soc Lond A 1975;343:461.
[30] Russell JH, Wallwork SC. Acta Crystallogr 1972;B28:1527.
[31] Mahmood MM, Wallwork SC. Acta Crystallogr 1976;B32:440.
[32] Russell JH, Wallwork SC. Acta Crystallogr 1969;B25:1691.
[33] Bukowska-Strzyzewska M, Tosik A. Pol J Chem 1979;53:2423.
[34] Poizat O, Sourisseau C, Corset J. J Molec Struct 1986:143;203.
[35] Hester RE, Suzuki S. J Phys Chem 1982;86:4626.